

## Preparation of hollow silica microsphere and its effect on the thermal conductivity of polymer composites

SHU Jingjing<sup>1</sup>, CHEN Jian<sup>1</sup>, CHEN Yawei<sup>2</sup>, ZHAO Chu<sup>1</sup>, WANG Mozhen<sup>1\*</sup>, GE Xuewu<sup>1\*</sup>

1. CAS Key Laboratory of Soft Matter Chemistry, Department of Polymer Science and Engineering, University of Science and Technology of China, Hefei 230026, China;

2. CAS Key Laboratory of Materials for Energy Conversion, Department of Materials Science and Engineering, University of Science and Technology of China, Hefei 230026, China

\* Corresponding author. E-mail: pstwmz@ustc.edu.cn; xwge@ustc.edu.cn

**Abstract:** The thermal conductivity of polymer composites filled with hollow microspheres is closely related to the content and structure of hollow microspheres. In this paper, micron-sized monodisperse polystyrene (PS) microspheres are synthesized as the sacrificial template to prepare a series of hollow SiO<sub>2</sub>(H-SiO<sub>2</sub>) microspheres with different inner and outer radius ratios ( $r/R$ ). The  $r/R$  value is controlled by the relative content of PS microspheres and tetraethyl orthosilicate (TEOS). The chemical composition and morphology of H-SiO<sub>2</sub> microspheres are characterized by infrared spectroscopy, scanning electron microscopy and transmission electron microscopy. Further, H-SiO<sub>2</sub> microspheres are blended with polydimethylsiloxane (PDMS) at a certain content to obtain H-SiO<sub>2</sub>/PDMS composite rubbers. The effect of the content and the  $r/R$  value of H-SiO<sub>2</sub> microspheres on the thermal conductivity of the composite rubber are investigated. Combined with the theoretical model calculation on the thermal conductivity of the silicone rubber, it can be concluded that the addition of H-SiO<sub>2</sub> microspheres with a complete hollow structure and an  $r/R$  value higher than 0.963 can reduce the thermal conductivity of H-SiO<sub>2</sub>/PDMS composite rubbers. The more the H-SiO<sub>2</sub> microspheres, the smaller the thermal conductivity of the composite rubber. At the same time, when the mass fraction of H-SiO<sub>2</sub> microspheres is no more than 5%, the mechanical properties of the H-SiO<sub>2</sub>/PDMS composite rubber are also enhanced with the increase of the weight content of H-SiO<sub>2</sub> microspheres. This work provides theoretical and experimental guidance for the design and preparation of high-performance hollow microspheres filled with polymer thermal insulation materials.

**Keywords:** hollow silica microspheres; silicone rubber; thermal conductivity; thermal insulation material  
**CLC number:** TB33      **Document code:** A

### 1 Introduction

With the rise of environmental protection concepts and the development of science and technology, thermal insulation materials have been widely used in various fields<sup>[1,2]</sup>, such as housing construction<sup>[3,4]</sup>, aircraft and aerospace equipment<sup>[5]</sup>, and mobile phones<sup>[6]</sup>. Thermal insulation materials must have a low thermal conductivity. For example, air has a thermal conductivity as low as  $0.0257 \text{ W} \cdot \text{m}^{-1} \cdot \text{K}^{-1}$ , resulting in an excellent thermal insulation performance. However, the thermal conductivity of organic and inorganic solid materials is much higher than that of air. Therefore, a special structural design is necessary to obtain a solid matrix with a low thermal conductivity.

The introduction of closed cavities inside the material, such as the formation of a porous foam structure with a large amount of air stored, can greatly reduce the thermal conductivity of the material<sup>[7-10]</sup>. This method has been widely used to prepare a variety of polymer-based thermal insulation materials<sup>[11]</sup>. However, the porous structure will make the mechanical properties of the matrix weakened, resulting in a poor toughness and low strength, thus limiting its practical application fields<sup>[12-16]</sup>. The addition of hollow structure fillers, such as hollow polymer microspheres<sup>[17]</sup>, hollow glass microspheres<sup>[18]</sup>, and hollow silica microspheres<sup>[19-22]</sup>, into the substrate is another alternative in order to obtain a composite material with low thermal conductivity and good mechanical properties. However, many theoretical

and practical research have shown that the addition of hollow microspheres doesn't always reduce the thermal conductivity of the matrix and increase its thermal insulation performance<sup>[23, 24]</sup>. In fact, the thermal conductivity of this kind of filled composite material is closely related to both the content and the structure of the hollow structure fillers<sup>[25, 26]</sup>. Therefore, the precise structural design on the hollow microspheres is the premise of their use as the filler in the preparation of thermal insulation materials.

Hollow silica (H-SiO<sub>2</sub>) microspheres are non-toxic and eco-friendly<sup>[27]</sup>, and possess good thermostability and mechanical properties, which are expected to be an ideal filler for the preparation of thermal insulation materials<sup>[28, 29]</sup>. Although there are myriads of studies on the preparation of H-SiO<sub>2</sub> microspheres<sup>[30, 31]</sup>, the correlation between the structure of the hollow microspheres (the microsphere size, the shell thickness, the surface structure and properties, etc.) and the thermal conductivity of the final composite has been rarely discussed. On the other hand, the mechanical properties of the particle-filled composite materials (such as the flexural strength and modulus, radial tensile strength, and fracture toughness) are also dependent on the particle size and content, as well as the area occupied by the particles<sup>[32]</sup>. Generally, nano-scaled fillers will have a much larger contact area with the matrix than micron-scaled filler at the same mass ratio, which can improve the mechanical properties of composite materials more efficiently<sup>[33-35]</sup>. However, the synthesis process of nano-scaled H-SiO<sub>2</sub> microspheres is more complicated, and it is also difficult to disperse nano-scaled H-SiO<sub>2</sub> microspheres uniformly in the polymer matrix. At the same time, as a filler of thermal insulation materials, the spherical shell is required to be as thin as possible to allow more air, which in turn makes the mechanical strength of the hollow microspheres worse. Therefore, a precise control of the size and the shell thickness of H-SiO<sub>2</sub> microspheres is required for the preparation of thermal insulation materials with excellent thermal insulation performance and better mechanical strength, which is a challenge in the synthesis of H-SiO<sub>2</sub> microspheres.

Silicone rubber materials such as polydimethylsiloxane (PDMS) have good electrical insulation and chemical stability<sup>[36-39]</sup>. They are often used as thermal insulation materials on aircraft and rocket engine components<sup>[5, 40]</sup> due to their inherent poor thermal conductivity (the thermal conductivity is 0.1519 W · m<sup>-1</sup> · K<sup>-1</sup>)<sup>[18]</sup>. However, the thermal conductivity of silica is as high as 1.3–1.5 W · m<sup>-1</sup> · K<sup>-1</sup><sup>[24]</sup>. Thus, how to identify an optimal size, shell thickness, and content of H-SiO<sub>2</sub> microspheres is the key problem for

the successful preparation of high-performance thermal insulation silicone rubber materials.

In this paper, micron-sized H-SiO<sub>2</sub> microspheres with different inner and outer radius ratios ( $r/R$ ) were prepared using the polystyrene (PS) microspheres as the sacrificial template. Then, the H-SiO<sub>2</sub> microspheres were blended with PDMS in different proportions to obtain H-SiO<sub>2</sub>/PDMS composite rubbers. The thermal conductivities of H-SiO<sub>2</sub>/PDMS composite rubbers were measured, and their dependence on the  $r/R$  value and the content of H-SiO<sub>2</sub> microspheres was investigated. Combined with the theoretical model calculation on the thermal conductivity of H-SiO<sub>2</sub>/PDMS composite rubbers, the addition of H-SiO<sub>2</sub> microspheres which have a complete hollow structure and an  $r/R$  value higher than 0.963 can reduce the thermal conductivity of H-SiO<sub>2</sub>/PDMS composite rubbers. At the same time, the mechanical properties of H-SiO<sub>2</sub>/PDMS composite rubbers are also enhanced. Therefore, this work provides theoretical and experimental guidance for the preparation of high-performance H-SiO<sub>2</sub>/PDMS thermal insulation materials.

## 2 Materials and methods

### 2.1 Materials

Methacrylateoethyltrimethyl ammonium chloride (MTC) aqueous solution (mass fraction 80%) was purchased from Bidepharm. Styrene (St), azobisisobutyronitrile (AIBN), polyvinyl pyrrolidone (PVP K30), tetraethyl orthosilicate (TEOS), ammonia, stannous octoate (Sn(Oct)<sub>2</sub>), and absolute ethanol were purchased from Sinopharm Chemical Reagent Co., Ltd. St and AIBN were refined by vacuum distillation and recrystallization respectively before use. Hydroxy-terminated polydimethylsiloxane (PDMS, viscosity: 2000 mm<sup>2</sup> · s<sup>-1</sup>) was purchased from Hubei Xinsihai Chemical Co., Ltd. Deionized water was used in all experiments.

### 2.2 Synthesis of hollow silica (H-SiO<sub>2</sub>) microspheres

H-SiO<sub>2</sub> microspheres were prepared by a sacrificial template method, as shown in Figure 1. First, monodispersed polystyrene (PS) template microspheres were synthesized according to the previous work of Wu et al.<sup>[41]</sup>. PVP (1.5 g) was ultrasonically dissolved in a mixture of 45 g of ethanol and 10 mL of water, followed by the addition of 10 g of St and 400 mg of AIBN under magnetic stirring. After being deoxygenated by bubbling nitrogen for 20 min, the system was heated to 70 °C and reacted for 1.5 h. A mixture of 45 g of ethanol, 0.5 g of MTC, and 10 g of St was added to the system, and the reaction continued for 14 h at 70 °C to obtain PS microspheres. Next, the system was cooled naturally to 50 °C, followed by the addition of 2 mL of ammonia and a certain amount of TEOS, then continued

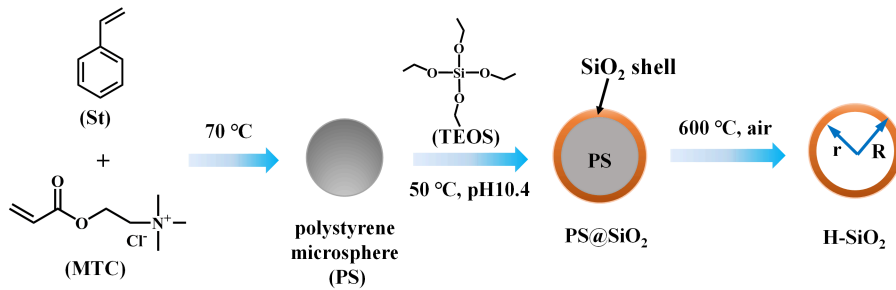


Figure 1. Preparation principle of H-SiO<sub>2</sub> microspheres.

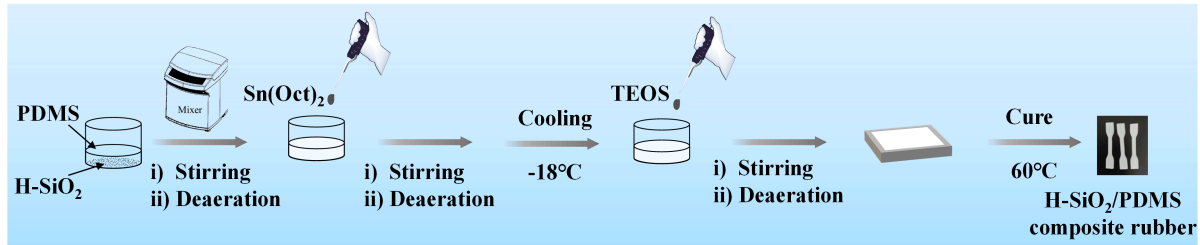


Figure 2. Preparation process of H-SiO<sub>2</sub>/PDMS composite rubber.

to react at 50 °C for 8 h to let the formation of a silica shell around PS microspheres (PS@SiO<sub>2</sub>). Finally, the PS@SiO<sub>2</sub> microspheres were separated by centrifugation (4000 r/min, 3 min), washed with ethanol, and dried in an oven at 60 °C to a constant weight, then calcinated at 600 °C in a muffle furnace for 5 h to obtain H-SiO<sub>2</sub> microspheres.

### 2.3 Preparation of H-SiO<sub>2</sub>/PDMS composite rubber

The preparation process of the H-SiO<sub>2</sub>/PDMS composite rubber is shown in Figure 2. Firstly, a certain amount of the as-prepared H-SiO<sub>2</sub> microspheres and PDMS were mixed in a homogenizer (THINKY ARE-310) by stirring at 1500 r/min for 5 min, and deaeration at 2200 r/min for 1 min. Next, Sn(Oct)<sub>2</sub> (0.5% of the mass of PDMS) was added. After the same stirring and degassing as above, the mixture was cooled at -18 °C in a refrigerator for 20 min. Then, TEOS (0.75% of the mass of PDMS) was added into the system. After being stirred and degassed again, the mixture was poured into a square plastic mold, degassed in vacuum for 10 min, and then cured in an oven at 60 °C for 6 h.

### 2.4 Characterizations for products

The morphology of the microspheres was characterized by a transmission electron microscope (TEM, JEOL2011 (H-7650), 100 kV) and a scanning electron microscope (SEM, JEOL (JSM-6700), 10 kV). The average particle size ( $D_n$ ), the weight-average particle size ( $D_w$ ) and the polydispersity index (PDI) of the microspheres were measured using the Adobe Photoshop CS3 software, and calculated according to the following equations with the diameters of at least 100 particles measured in the SEM images.

$$D_n = \frac{\sum n_i D_i}{\sum n_i} \quad (1)$$

$$D_w = \frac{\sum n_i D_i^4}{\sum n_i D_i^3} \quad (2)$$

$$PDI = \frac{D_w}{D_n} \quad (3)$$

Where  $n_i$  is the number of the microspheres with a diameter of  $D_i$ .

The infrared spectra of PS, PS@SiO<sub>2</sub> and H-SiO<sub>2</sub> were performed on attenuated total reflectance-Fourier transform infrared spectroscopy (ATR-FTIR, ALPHA II) in a range of 400–4000 cm<sup>-1</sup> with a resolution of 2 cm<sup>-1</sup> and 96 overlay scans.

The thermal conductivity of the composite rubber was measured by the thermal conductivity meter (Hot Disk 2500s) at 25 °C. Three cylindrical specimens with a diameter of 50 mm ± 1 mm and a thickness of 30 mm ± 1 mm were cut out for each sample. The thermal conductivity of the sample is the average of the measured thermal conductivities of the three specimens. The tensile properties of the composite silicone rubber were characterized on the electronic universal testing machine (UTM2502) with a crosshead rate of 10 (mm · min<sup>-1</sup>) according to GB/T528-2009. The tested specimens were dumbbell-shaped with the width of the narrow middle part of 4 mm ± 0.2 mm and the thickness of 2 mm ± 0.2 mm. Five specimens were tested for each composite rubber sample. The tensile strength and elongation at break of the specimens were recorded and averaged as the tensile strength and the elongation at

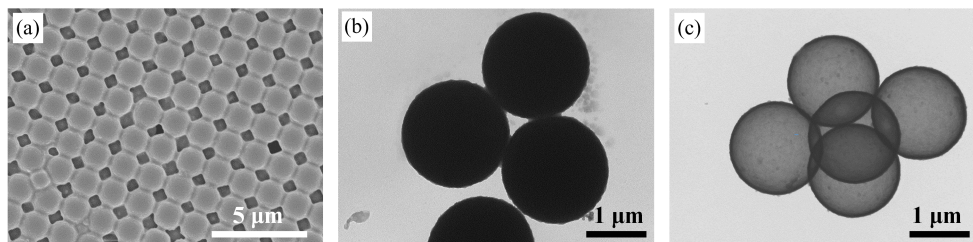


**Figure 3.** SEM image of PS microspheres (a), TEM images of PS@SiO<sub>2</sub> microspheres (b) and H-SiO<sub>2</sub> microspheres (c) prepared by the calcination of the sample in (b). (The sample in (b) was prepared at a condition of the relative feed volume of TEOS to St ( $V_{\text{TEOS}} : V_{\text{St}}$ ) of 0.7 : 2.2.).

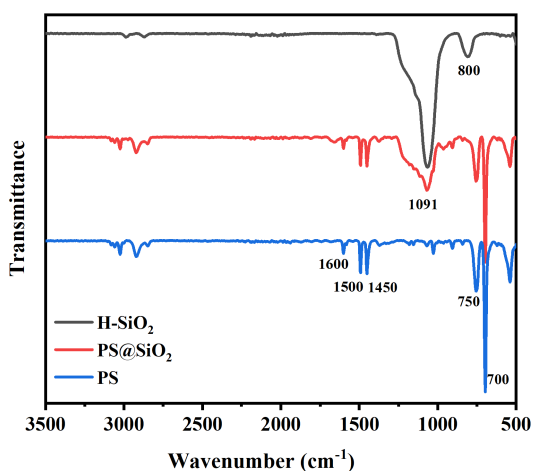


**Figure 4.** IR spectra of PS, PS@SiO<sub>2</sub> and H-SiO<sub>2</sub> microspheres.

break of the sample.

### 3 Results and discussion

#### 3.1 Preparation and morphology control of H-SiO<sub>2</sub> microspheres

In this work, monodispersed PS microspheres were prepared by the dispersion polymerization of St and a small amount of comonomer MTC in an aqueous alcohol solution using PVP as the dispersant. The morphology of the PS microspheres is shown in Figure 3(a). The average particle size and PDI of PS microspheres are 1.4 μm and 1.001 respectively.

The infrared spectrum of PS microspheres is shown in Figure 4, on which the characteristic absorption peaks of the benzene ring skeleton (1450 cm<sup>-1</sup>, 1500 cm<sup>-1</sup>, 1600 cm<sup>-1</sup>) can be clearly seen. The bands at 700 cm<sup>-1</sup> and 750 cm<sup>-1</sup> are identified as the deformation vibration absorption peaks of the C-H bonds on the monosubstituted benzene ring.

Obviously, the water-soluble PVP and hydrophilic quaternary ammonium ions are distributed on the surface of the PS microspheres, which is conducive to the adsorption of TEOS and its hydrolysate on the surface of the PS template microspheres<sup>[42-44]</sup>. So a silica layer can

be coated on the PS microsphere to obtain the PS@SiO<sub>2</sub> composite microsphere, as shown in Figure 1. Figure 3 (b) displays a typical TEM image of PS@SiO<sub>2</sub> composite microspheres, which are obtained at a condition of relative feed volume of TEOS to St ( $V_{\text{TEOS}} : V_{\text{St}}$ ) of 0.7 : 2.2. It can be observed that the shape of the microspheres hardly changed after the coating of the silica layer except that the diameter of PS@SiO<sub>2</sub> microsphere increases slightly to 1.75 μm. The infrared spectrum of PS@SiO<sub>2</sub> composite microspheres is shown in Figure 4. In addition to the characteristic absorption peaks of PS, a strong and broad absorption band around 1091 cm<sup>-1</sup> assigned to the anti-stretching vibration of Si-O-Si occurs, indicating the presence of SiO<sub>2</sub> in the prepared PS@SiO<sub>2</sub> microspheres. After being calcinated at high temperature, the solid PS@SiO<sub>2</sub> composite microspheres are transformed into H-SiO<sub>2</sub> microspheres, as shown in Figure 3 (c). The striking contrast between the edge and the middle of H-SiO<sub>2</sub> microspheres indicate a typical hollow structure. At the same time, the characteristic absorption peaks of silica can be seen in the infrared spectrum of the H-SiO<sub>2</sub> microspheres in Figure 4 (the peak at 800 cm<sup>-1</sup> can be identified as the symmetric stretching vibration of Si-O bonds), and the characteristic absorption peaks of PS nearly disappeared, indicating that H-SiO<sub>2</sub> microspheres are successfully prepared.

The shell thicknesses of the H-SiO<sub>2</sub> microspheres are controlled by adjusting the relative content of TEOS and PS microspheres. Figure 5 shows the morphologies of H-SiO<sub>2</sub> microspheres prepared at different  $V_{\text{TEOS}} : V_{\text{St}}$ . The corresponding structure parameters of the H-SiO<sub>2</sub> microspheres are listed in Table 1. It can be seen that the shell thickness of H-SiO<sub>2</sub> increases with the relative amount of TEOS. When the relative amount of TEOS is low, i. e.,  $V_{\text{TEOS}} : V_{\text{St}} = 0.6 : 2.2$  (Figure 5 (a1-a3)), a large number of broken H-SiO<sub>2</sub> microspheres can be observed. It means that when the relative amount of TEOS is small, it is not enough to form a complete silica shell on the surface of all PS template microspheres. Therefore, broken silica shells

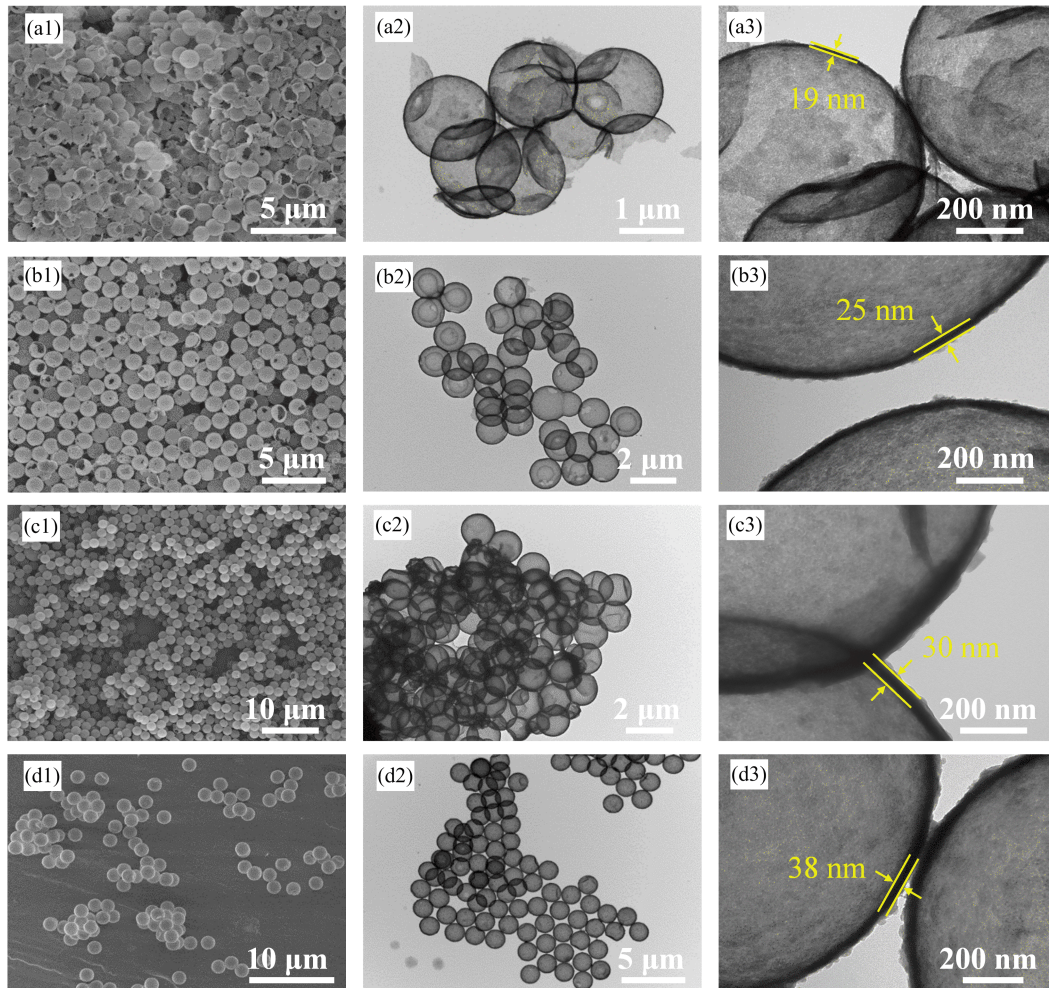


**Figure 5.** SEM (a1–d1) and TEM (a2–d2) images of H-SiO<sub>2</sub> microspheres prepared at different  $V_{\text{TEOS}} : V_{\text{St}}$ . (a1–a3) : 0.6 : 2.2; (b1–b3) : 0.7 : 2.2; (c1–c3) : 0.8 : 2.2; (d1–d3) : 0.9 : 2.2. a3–d3 are the enlarged TEM images of the corresponding a2–d2.

are left after the inner PS cores are removed by calcination. When  $V_{\text{TEOS}} : V_{\text{St}} \geq 0.7 : 2.2$ , almost all the surface of PS microspheres can be covered by silica, thus H-SiO<sub>2</sub> microspheres with complete morphology can be obtained. However, the diameter of the cavity (1.4 μm) of the obtained H-SiO<sub>2</sub> microspheres is unchanged with the TEOS content, which is consistent with the diameter of the PS template microsphere.

**Table 1.** The structure parameters of H-SiO<sub>2</sub> microspheres prepared at different  $V_{\text{TEOS}} : V_{\text{St}}$ .

Sample ID	$V_{\text{TEOS}} : V_{\text{St}}$	$r^*/\text{nm}$	$R^{**}/\text{nm}$	$r/R$	Shell thickness /nm
1	0.6 : 2.2	700	719	0.974	19
2	0.7 : 2.2	700	725	0.966	25
3	0.8 : 2.2	700	730	0.959	30
4	0.9 : 2.2	700	738	0.948	38

[ Note ] \* inner radius of H-SiO<sub>2</sub> microspheres; \*\* outer radius of H-SiO<sub>2</sub> microspheres

### 3.2 The influence of the content and the structure of H-SiO<sub>2</sub> microsphere on the thermal conductivity of H-SiO<sub>2</sub>/PDMS composite

The as-prepared H-SiO<sub>2</sub> microspheres and PDMS were uniformly mixed in a certain proportion, then a small amount of TEOS was added as the crosslinking agent to form H-SiO<sub>2</sub>/PDMS composite rubber under the catalysis of Sn(Oct)<sub>2</sub>. When the mass fraction of H-SiO<sub>2</sub> microspheres is no more than 5%, they have good dispersibility in PDMS without any agglomerations, as shown in the SEM images of the cross-section of the composite silicone rubbers in Figure 6. Moreover, the hollow microspheres have a certain strength since no deformation or fragmentation can be observed during the mixing and curing process. These indicate that the as-prepared H-SiO<sub>2</sub> microspheres have enough structure stability and good compatibility with PDMS, which make them be used as a promising filler to prepare composite silicone rubbers with good performance.

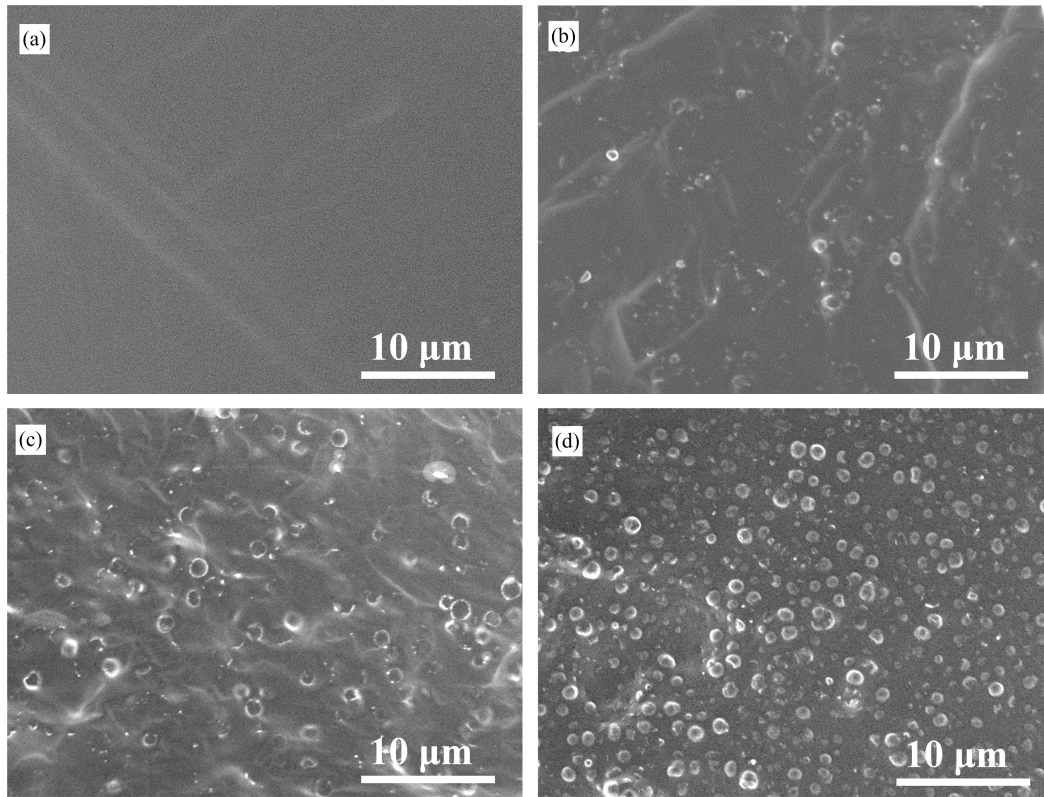


**Figure 6.** The SEM images of the fracture surfaces of H-SiO<sub>2</sub>/PDMS with different mass fraction of H-SiO<sub>2</sub>: (a) 0% , (b) 1% , (c) 3% , and (d) 5% . (Samples were brittle broken after being immersed in liquid nitrogen for 20 min).

Many studies on the theoretical calculation on the influence of the content and structural parameters of hollow microsphere on the thermal conductivity of composite materials have been reported<sup>[11, 23]</sup>. The heat conduction process of the hollow microspheres filled polymer composite material includes: ① the heat conduction process of the solid matrix of the composite material and the gas inside the microsphere; ② the heat radiation process of the solid; ③ the gas convection process in the microsphere. It is generally believed that the heat radiation process ② can be ignored when the temperature is not too high. In addition, the process ③ does not need to be considered, since the gas cannot undergo convection in small microspheres. Therefore, only the heat conduction processes of each solid material and gas are used to calculate the overall thermal conductivity of the material. According to the principle of minimum thermal resistance and the assumption that the specific equivalent thermal conductivity is equal, Liang et al.<sup>[46, 47]</sup> deduced that the equivalent thermal conductivity ( $k_{eff}$ ) of polymer composite materials filled with the hollow microspheres could be calculated by the following Equation (4):

$$k_{eff} = \frac{1}{k_p} \left[ 1 - \frac{6\varphi_f}{\pi} \left( \frac{1}{3} \right)^{\frac{1}{3}} \right] + 2 k_p \frac{4\pi}{3\varphi_f} \left( \frac{1}{3} \right)^{\frac{1}{3}} +$$

$$\pi \frac{2\varphi_f}{9\pi} \left( \frac{1}{3} \right)^{\frac{1}{3}} \left[ k_g \frac{\rho_s - \rho_a}{\rho_g - \rho_a} + k_a \frac{\rho_g - \rho_s}{\rho_g - \rho_a} - k_p \right] \left( \frac{r}{R} \right)^3 \left( \frac{1}{3} \right)^{\frac{1}{3}} \quad (4)$$

Where  $k_p$ ,  $k_g$ , and  $k_a$  are the thermal conductivities of the polymer matrix, the shell of the filled microsphere and the gas in the microsphere, respectively.  $\varphi_f$  is the volume fraction of the filled microsphere.  $\rho_s$ ,  $\rho_g$ , and  $\rho_a$  are the equivalent density of the microsphere, the shell density, and the density of the gas in the microsphere, respectively.  $\rho_s$  is defined as

$$\rho_s = \frac{\rho_g V_g}{V_s} = \rho_g \left[ 1 - \frac{r}{R} \right]^3 \quad (5)$$

where  $V_g$  and  $V_s$  are the volumes of the spherical shell and the entire microsphere, and  $r$  and  $R$  are the inner and outer radii of the hollow microsphere. The gas density  $\rho_a$  is negligible compared with  $\rho_s$  and  $\rho_g$ , that is,  $\rho_s - \rho_a \approx \rho_s$ ,  $\rho_g - \rho_a \approx \rho_g$ . After simplification, Equation (4) can be expressed as

$$k_{eff} = \frac{1}{k_p} \left[ 1 - \frac{6\varphi_f}{\pi} \left( \frac{1}{3} \right)^{\frac{1}{3}} \right] + 2 k_p \frac{4\pi}{3\varphi_f} \left( \frac{1}{3} \right)^{\frac{1}{3}} + \pi \frac{2\varphi_f}{9\pi} \left( \frac{1}{3} \right)^{\frac{1}{3}} \left[ k_g - k_p + (k_a - k_g) \frac{r}{R} \right] \left( \frac{1}{3} \right)^{\frac{1}{3}} \quad (6)$$

Generally, the hollow microspheres are added to the matrix based on the mass fraction ( $w$ ). Thus,  $\varphi_f$  can be

calculated from  $w$  according to the following Equation (7):

$$\varphi_f = \frac{\frac{wM}{\rho_s}}{\frac{wM}{\rho_s} + \frac{(1-w)M}{\rho_p}} = \frac{1}{1 + \frac{1}{w} - 1} \left[ 1 - \frac{r}{R} \left( \frac{\rho_g}{\rho_p} \right)^{-1} \right] \quad (7)$$

where  $M$  is the total mass of the composite material,  $w$  is the mass fraction of the filled microspheres, and  $\rho_p$  is the density of the polymer matrix. The  $k_{\text{eff}}$  of the composite material can be calculated from Equations (6) and (7). For the H-SiO<sub>2</sub>/PDMS composite rubber, the required parameters are listed as follows:  $k_p = 0.1519 \text{ W} \cdot \text{m}^{-1} \cdot \text{K}^{-1}$  (measured by experiment),  $k_g = 1.4 \text{ W} \cdot \text{m}^{-1} \cdot \text{K}^{-1}$ <sup>[30]</sup>,  $k_a = 0.0257 \text{ W} \cdot \text{m}^{-1} \cdot \text{K}^{-1}$ ,  $\rho_p = 0.97 \text{ g} \cdot \text{cm}^{-3}$ ,  $\rho_g = 2.32 \text{ g} \cdot \text{cm}^{-3}$ . By substituting them into Equations (6) and (7), the dependence of  $k_{\text{eff}}$  of the composite rubbers with different H-SiO<sub>2</sub> mass fraction ( $w = 1\%$ ,  $3\%$ , and  $5\%$ ) on  $r/R$  of the hollow microspheres can be theoretically calculated, as shown by the solid lines in Figure 7. It can be seen that when  $r/R = 0.963$ , no matter how much H-SiO<sub>2</sub> microspheres added, the thermal conductivity of the composite rubber is as same as that of the pure PDMS matrix, in other words,  $k_{\text{eff}} = k_p$ . These results can also be deduced from Equation (6), when  $k_{\text{eff}} = k_p$ :

$$\frac{r}{R} \left( \frac{\rho_g}{\rho_p} \right)^{-1} = \frac{k_g - k_p}{k_g - k_a} = 0.892 \Rightarrow \frac{r}{R} = 0.963 \quad (8)$$

When  $r/R < 0.963$ , the addition of H-SiO<sub>2</sub> microspheres can only increase the thermal conductivity of the composite rubber. The more the H-SiO<sub>2</sub> microspheres

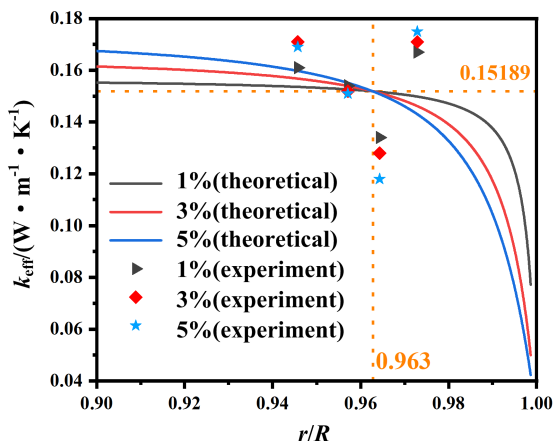


**Figure 7.** The relationship between the theoretical equivalent thermal conductivities (solid lines) and the measured thermal conductivities (symbols) of the H-SiO<sub>2</sub>/PDMS composite rubber with different H-SiO<sub>2</sub> mass fraction and the  $r/R$  of H-SiO<sub>2</sub>.

added, the higher the thermal conductivity. Only when  $r/R > 0.963$ , the addition of H-SiO<sub>2</sub> microspheres can reduce the thermal conductivity of the composite rubber. The more the H-SiO<sub>2</sub> microspheres added, the smaller the thermal conductivity of the composite rubber.

The actual thermal conductivity of H-SiO<sub>2</sub>/PDMS composite rubber was measured by the thermal constant analyzer, as shown by the data points of different colors in Figure 7. It can be seen that when the H-SiO<sub>2</sub> microspheres with  $r/R$  of 0.948 ( $< 0.963$ ) are used, the actual thermal conductivity of the composite rubber is indeed higher than that of the silicone rubber matrix, and increase with the content of H-SiO<sub>2</sub> microspheres. The thermal conductivity of H-SiO<sub>2</sub>/PDMS composite rubber prepared from H-SiO<sub>2</sub> microspheres with  $r/R$  of 0.958 (less but close to 0.963) is close to that of pure PDMS matrix. The thermal conductivity of H-SiO<sub>2</sub>/PDMS composite rubber prepared by H-SiO<sub>2</sub> microspheres with  $r/R$  of 0.966 ( $> 0.963$ ) is less than that of the silicone rubber matrix. And the more the H-SiO<sub>2</sub> microspheres, the smaller the thermal conductivity of the composite rubber. When the mass fraction of H-SiO<sub>2</sub> microspheres reaches 5%, the thermal conductivity of the sample is only  $0.118 \text{ W} \cdot \text{m}^{-1} \cdot \text{K}^{-1}$ , which is 22.3% lower than that of the PDMS matrix. However, the thermal conductivity of H-SiO<sub>2</sub>/PDMS composite rubber prepared by adding H-SiO<sub>2</sub> microspheres with an  $r/R$  value of 0.974 is surprisingly increased. This can be attributed to that a large amount of broken silica shells exist in this case, as shown in Figure 5(a1-a3), which means the actual gas volume introduced by the addition of H-SiO<sub>2</sub> microspheres is much less than the theoretical prediction. The high thermal conductivity of silica itself ( $1.4 \text{ W} \cdot \text{m}^{-1} \cdot \text{K}^{-1}$ ) leads to the thermal conductivity of the final composite rubber is much higher than the theoretical prediction.

In summary, in order to achieve much lower thermal conductivity of the H-SiO<sub>2</sub>/PDMS composite rubber, H-SiO<sub>2</sub> microspheres should have a complete hollow structure and an  $r/R$  value higher than 0.963. The more the H-SiO<sub>2</sub> microspheres, the smaller the thermal conductivity of the composite rubber, which further improves the thermal insulation performance of the composite rubber.

### 3.3 Mechanical properties of the H-SiO<sub>2</sub>/PDMS composite rubber

The mechanical properties of the H-SiO<sub>2</sub>/PDMS composite rubber directly affect its application prospects. The tensile strength and elongation at break of the silicone rubber filled with different contents of H-SiO<sub>2</sub> microspheres ( $r/R$  of 0.966) were characterized, as shown in Figure 8. When the mass fraction of H-SiO<sub>2</sub> microspheres is no more than 5%, the tensile

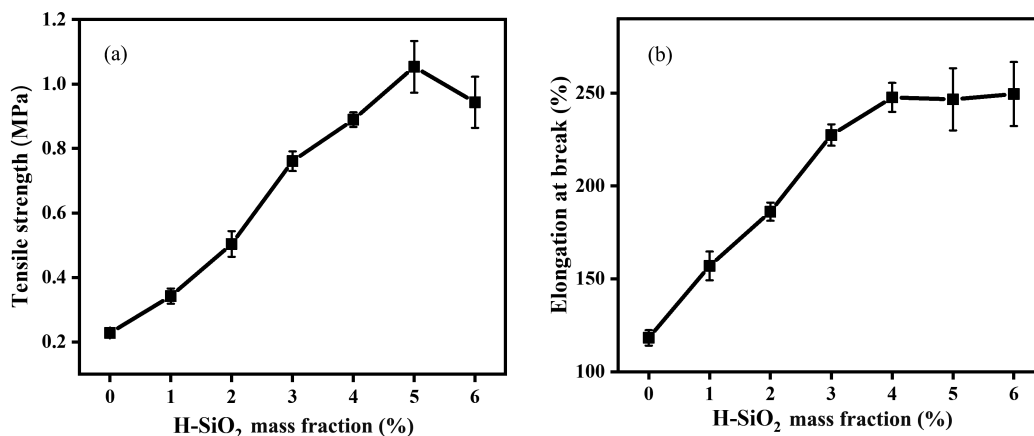


**Figure 8.** The relationship between (a) the tensile strength, (b) elongation at break of H-SiO<sub>2</sub>/PDMS silicone composite rubber and the weight content of H-SiO<sub>2</sub>.

strength and the corresponding elongation at break of the composite rubber increase with the weight content of H-SiO<sub>2</sub> microspheres, indicating that the mechanical properties of the composite rubber have been significantly improved. When the mass fraction of H-SiO<sub>2</sub> is 5%, the tensile strength of the H-SiO<sub>2</sub>/PDMS composite rubber is 1.05 MPa, which is 4.6 times that of pure silicone rubber (0.23 MPa). At the same time, its elongation at break reaches ~250%, which is more than twice of that of the pure silicone rubber (120%). It has been reported in the literature that the mechanical properties of the composite will be deteriorated when hollow glass beads with a larger particle size (10–100 μm) are filled in the silicone rubber<sup>[45]</sup>. It means a smaller size of the hollow silica microspheres will be helpful to improve the mechanical properties of the composite rubber. However, when the mass fraction of H-SiO<sub>2</sub> increases to more than 5%, the elongation at break of the composite rubber changes little, but the tensile strength has an obvious decrease with the increase of the content of H-SiO<sub>2</sub>. This indicates that excessive H-SiO<sub>2</sub> microspheres may hinder the formation of the cross-linked network of the silicone rubber, thereby reducing the toughness of the composite rubber. Therefore, in order to prepare composite rubber with low thermal conductivity and good mechanical properties, it is best to use the H-SiO<sub>2</sub> microspheres with a complete hollow structure and an  $r/R$  value higher than 0.963. At the same time, the mass fraction of the H-SiO<sub>2</sub> microspheres is preferably no more than 5%.

## 4 Conclusions

In this paper, a series of monodisperse H-SiO<sub>2</sub> microspheres (~1.4 μm) with different inner and outer radius ratios ( $r/R$ ) were synthesized using the PS

microspheres as the sacrificial templates. The as-prepared H-SiO<sub>2</sub> microspheres have good compatibility with PDMS, and can be dispersed homogeneously in PDMS to obtain H-SiO<sub>2</sub>/PDMS composite rubbers. The thermal conductivities of the composite rubbers with different content and  $r/R$  value of H-SiO<sub>2</sub> microspheres were measured. Combined with the theoretical calculation, it confirms that only the addition of H-SiO<sub>2</sub> microspheres with complete hollow structure and an  $r/R$  value higher than 0.963 can make the thermal conductivity of the H-SiO<sub>2</sub>/PDMS composite rubber lower than that of the pure PDMS matrix. At the same time, when the mass fraction of the micron-sized H-SiO<sub>2</sub> microspheres is no more than 5%, the mechanical properties of the H-SiO<sub>2</sub>/PDMS composite rubber can also be enhanced as the increase of the mass fraction of H-SiO<sub>2</sub> microspheres. At present, the thermal conductivity of the commercial solid insulation silicone rubber materials ranges from 0.15 to 0.25 W · m<sup>-1</sup> · K<sup>-1</sup>. Thus, the H-SiO<sub>2</sub>/PDMS composite rubber prepared in this work not only has a much lower and adjustable thermal conductivity, but also an improved mechanical property. This work provides theoretical and experimental guidance for the preparation of high-performance polymer thermal insulation materials filled with hollow microspheres.

## Acknowledgments

This work is supported by the Fundamental Research Funds for the Central Universities (WK9110000066, WK3450000005, WK3450000006), and the National Natural Science Foundation of China (51973205, 51573174, 51773189).

## Conflict of interest

The authors declare no conflict of interest.



## Author information

**SHU Jingjing** studied at the Department of Polymer Science and Engineering in the University of Science and Technology of China under the supervision of Assoc. Prof. Wang Mozhen and Prof. Ge Xuewu. She received her master's degree in June 2021. Her research mainly focuses on the preparation of porous silica materials.

**WANG Mozhen** (corresponding author) received her PhD in Polymer Chemistry and Physics from the University of Science and Technology of China (USTC). She is currently an associate professor at the Department of Polymer Science and Engineering, USTC. Her research interests include the fabrication of nano/micro-structured materials with controllable morphology and structure, such as porous and hollow polymeric microspheres, anisotropic particles and organic/inorganic nanocomposites.

**GE Xuewu** (corresponding author) received his master's degree from the University of Science and Technology of China (USTC). He is currently a professor at the Department of Polymer Science and Engineering, USTC. His research interests include the mechanism and application of radiation chemistry principles, and the fabrication of nano/micro-structured materials.

## References

- [1] Apostolopoulou K V, Munier P, Bergström L. Thermally insulating nanocellulose-based materials. *Advanced Materials*, 2020; 2001839; doi:10.1002/adma.202001839.
- [2] Rajaei S, Shoaei P, Shariati M, et al. Rubberized alkali-activated slag mortar reinforced with polypropylene fibres for application in lightweight thermal insulating materials. *Construction and Building Materials*, 2021, 270; 121430.
- [3] Jelle B P. Traditional, state-of-the-art and future thermal building insulation materials and solutions: Properties, requirements and possibilities. *Energy and Buildings*, 2011, 43(10); 2549–2563.
- [4] Berardi U, Naldi M. The impact of the temperature dependent thermal conductivity of insulating materials on the effective building envelope performance. *Energy and Buildings*, 2017, 144; 262–275.
- [5] Kourtides D A. Thermal performance of composite flexible blanket insulations for hypersonic aerospace vehicles. *Composites Engineering*, 1993, 3(7); 805–813.
- [6] Sun Z Q, Lu C, Fan J M, et al. Porous silica ceramics with closed-cell structure prepared by inactive hollow spheres for heat insulation. *Journal of Alloys and Compounds*, 2016, 662; 157–164.
- [7] Ji X F, Zhang H, Bai Z, et al. Self-assembled multifunctional bulk hollow microspheres: Thermal insulation, sound absorption and fire resistance. *Energy and Buildings*, 2019, 205; 109533.
- [8] Zhang C L, Zhang C Y, Huang R, et al. Effects of hollow microspheres on the thermal insulation of polysiloxane foam. *Journal of Applied Polymer Science*, 2017, 134(18); 46025.
- [9] Wicklein B, Kocjan A, German S A, et al. Thermally insulating and fire-retardant lightweight anisotropic foams based on nanocellulose and graphene oxide. *Nature Nanotechnology*, 2015, 10(3); 277–283.
- [10] Zhao S, Malfait W J, Guerrero A N, et al. Biopolymer aerogels and foams: Chemistry, properties, and applications. *Angewandte Chemie International Edition*, 2018, 57(26); 7580–7608.
- [11] Hu F, Wu S Y, Sun Y G. Hollow-structured materials for thermal insulation. *Advanced Materials*, 2019, 31(38); 1801001.
- [12] Gao J, Wang J B, Xu H Y, et al. Preparation and properties of hollow glass bead filled silicone rubber foams with low thermal conductivity. *Materials & Design*, 2013, 46; 491–496.
- [13] Zhang X Z, Wang Y M, Ma L Y, et al. Ultra-light, heat-resistant, flexible and thermal insulation graphene-fluororubber foam prepared by using N<sub>2</sub> as a blowing agent. *Colloids and Surfaces A: Physicochemical and Engineering Aspects*, 2020, 604; 125310.
- [14] Zhang X Z, Wang C, Wang S, et al. A lightweight, thermal insulation and excellent weatherability foam crosslinked by electron beam irradiation. *Radiation Physics and Chemistry*, 2020, 173; 108890.
- [15] Zhang C Y, Qu L J, Wang Y N, et al. Thermal insulation and stability of polysiloxane foams containing hydroxyl-terminated polydimethylsiloxanes. *RSC Advances*, 2018, 8(18); 9901–9909.
- [16] Phiri M M, Sibeko M A, Phiri M J, et al. Effect of free foaming and pre-curing on the thermal, morphological and physical properties of reclaimed tyre rubber foam composites. *Journal of Cleaner Production*, 2019, 218; 665–672.
- [17] Kim C B, You N H, Goh M. Hollow polymer microcapsule embedded transparent and heat-insulating film. *RSC Advances*, 2018, 8(17); 9480–9486.
- [18] Zhao X W, Zang C G, Sun Y L, et al. Effect of hybrid hollow microspheres on thermal insulation performance and mechanical properties of silicone rubber composites. *Journal of Applied Polymer Science*, 2018, 135(11); 46025.
- [19] Ernawati L, Ogi T, Balgis R, et al. Hollow silica as an optically transparent and thermally insulating polymer additive. *Langmuir*, 2016, 32(1); 338–345.
- [20] Fiedler T, Öchsner A. On the thermal conductivity of adhesively bonded and sintered hollow sphere structures (HSS). *Materials Science Forum*, 2007, 553; 39–44.
- [21] Ng S, Jelle B P, Sandberg L I, et al. Hollow silica nanospheres as thermal insulation materials for construction: Impact of their morphologies as a function of synthesis pathways and starting materials. *Construction and Building Materials*, 2018, 166; 72–80.
- [22] Bao Y, Guo R Y, Ma J Z. Hierarchical flower-like hollow SiO<sub>2</sub>@TiO<sub>2</sub> spheres with enhanced thermal insulation and ultraviolet resistance performances for building coating. *ACS Applied Materials & Interfaces*, 2020, 12(21); 24250–24261.
- [23] Sharma J, Polizos G. Hollow silica particles: Recent progress and future perspectives. *Nanomaterials*, 2020, 10(8); 1599.
- [24] Bao Y, Kang Q L, Ma J Z. Structural regulation of hollow spherical TiO<sub>2</sub> by varying titanium source amount and their thermal insulation property. *Colloids and Surfaces A: Physicochemical and Engineering Aspects*, 2018, 537; 69–75.
- [25] Gao T, Jelle B P, Sandberg L I C, et al. Monodisperse

- hollow silica nanospheres for nano insulation materials; Synthesis, characterization, and life cycle assessment. *ACS Applied Materials & Interfaces*, 2013, 5(3): 761–767.
- [26] Grandcolas M, Jasinski E, Gao T, et al. Preparation of low density organosilica monoliths containing hollow silica nanospheres as thermal insulation materials. *Materials Letters*, 2019, 250: 151–154.
- [27] Yang W X, Xu G Q, Shu J J, et al. Preparation and adsorption property of novel inverse-opal hierarchical porous N-doped carbon microspheres. *Chinese Chemical Letters*, 2021, 32(2): 866–869.
- [28] Bao Y, Shi C H, Wang T, et al. Recent progress in hollow silica; Template synthesis, morphologies and applications. *Microporous and Mesoporous Materials*, 2016, 227: 121–136.
- [29] Nandiyanto A B D, Akane Y, Ogi T, et al. Mesopore-free hollow silica particles with controllable diameter and shell thickness via additive-free synthesis. *Langmuir*, 2012, 28(23): 8616–8624.
- [30] Zhang Y, Hsu B Y W, Ren C, et al. Silica-based nanocapsules: Synthesis, structure control and biomedical applications. *Chemical Society Reviews*, 2015, 44(1): 315–335.
- [31] Jiang M, Shu J J, Jin H Q, et al. Radiation-grafting modification of hollow mesoporous silica microspheres and their application in anti-corrosive coatings. *Journal of Radiation Research and Radiation Processing*, 2019, 37(5): 050203.
- [32] Kim K H, Ong J L, Okuno O. The effect of filler loading and morphology on the mechanical properties of contemporary composites. *The Journal of Prosthetic Dentistry*, 2002, 87(6): 642–649.
- [33] Crosby A J, Lee J Y. Polymer nanocomposites; The “nano” effect on mechanical properties. *Polymer Reviews*, 2007, 47(2): 217–229.
- [34] Syabani M W, Amaliyana I, Hermiyati I, et al. Silica from geothermal waste as reinforcing filler in artificial leather. *Key Engineering Materials*, 2020, 849: 78–83.
- [35] Wang H, Murray V J, Qian M, et al. Resistance of nanoclay reinforced epoxy composites to hyperthermal atomic oxygen attack. *Chinese Journal of Chemical Physics*, 2019, 32(5): 543–552.
- [36] Du B X, Ma T T, Su J G, et al. Effects of temperature gradient on electrical tree growth and partial discharge in silicone rubber under AC voltage. *IEEE Access*, 2020, 8: 54009–54018.
- [37] Zhan X B, Cai X Q, Zhang J Y. A novel crosslinking agent of polymethyl (ketoxime) siloxane for room temperature vulcanized silicone rubbers: Synthesis, properties and thermal stability. *RSC Advances*, 2018, 8(23): 12517–12525.
- [38] Yang K Q, Tang M. Three-dimensional phase evolution and stress-induced non-uniform Li intercalation behavior in lithium iron phosphate. *Journal of Materials Chemistry A*, 2020, 8(6): 3060–3070.
- [39] Wang Z G, Zhang X H, Wang F Q, et al. Chemical characterization and research on the silicone rubber material used for outdoor current transformer insulation. *Phosphorus, Sulfur, and Silicon and the Related Elements*, 2017, 192(1): 109–112.
- [40] Kim E S, Kim E J, Shim J H, et al. Thermal stability and ablation properties of silicone rubber composites. *Journal of Applied Polymer Science*, 2008, 110(2): 1263–1270.
- [41] Chen M, Wu L M, Zhou S X, et al. A method for the fabrication of monodisperse hollow silica spheres. *Advanced Materials*, 2006, 18(6): 801–806.
- [42] Zhang Q, Ge J P, Goebel J, et al. Rattle-type silica colloidal particles prepared by a surface-protected etching process. *Nano Research*, 2009, 2(7): 583–591.
- [43] Tao C Y, Yan H W, Yuan X D, et al. Sol-gel based antireflective coatings with superhydrophobicity and exceptionally low refractive indices built from trimethylsilanized hollow silica nanoparticles. *Colloids and Surfaces A: Physicochemical and Engineering Aspects*, 2016, 509: 307–313.
- [44] Duan G W, Xie L Z, Zhao C, et al. Influence of the surface electrical property of polymer template microspheres on the morphology of hollow silica microspheres. *Acta Polymerica Sinica*, 2017(5): 785–792.
- [45] Hu Y, Mei R G, An Z G, et al. Silicon rubber/hollow glass microsphere composites; Influence of broken hollow glass microsphere on mechanical and thermal insulation property. *Composites Science and Technology*, 2013, 79: 64–69.
- [46] Liang J Z, Li F X. Theoretical model of heat transfer model for polymer/hollow micro-sphere composites. *Journal of South China University Technology*, 2005, 33(10): 34–37.
- [47] Liang J Z, Li F X. Experimental verification of theoretical heat-transfer model of polymer/hollow microsphere composite. *Journal of South China University Technology*, 2006, 34(1): 114–116.

# 中空二氧化硅微球的制备及其对聚合物复合材料导热系数的影响

舒晶晶<sup>1</sup>, 陈剑<sup>1</sup>, 陈亚威<sup>2</sup>, 赵楚<sup>1</sup>, 汪谟贞<sup>1\*</sup>, 葛学武<sup>1\*</sup>

1. 中国科学院软物质化学重点实验室, 中国科学技术大学高分子科学与工程系, 安徽合肥 230026;

2. 中国科学院能量转换材料重点实验室, 中国科学技术大学材料科学与工程系, 安徽合肥 230026

\* 通讯作者. E-mail: pstwmz@ustc.edu.cn; xwge@ustc.edu.cn

**摘要:** 中空微球/聚合物复合材料的热导系数与中空微球的含量和结构密切相关. 本文以微米级单分散聚苯乙烯(PS)微球为牺牲模板, 通过调控 PS 微球和正硅酸四乙酯(TEOS)的相对含量, 制备了一系列表面包覆不同厚度 SiO<sub>2</sub> 的 PS@SiO<sub>2</sub> 核壳结构微球, 用高温煅烧去除 PS 模板后, 得到不同球壁内外径比( $r/R$ )的中空 SiO<sub>2</sub> (H-SiO<sub>2</sub>)微球. 通过红外光谱、扫描和透射电子显微镜等对 H-SiO<sub>2</sub> 微球的化学成分和形貌进行了表征, 并进一步测定了不同含量和  $r/R$  的 H-SiO<sub>2</sub> 与聚二甲基硅氧烷(PDMS)复合后得到的 H-SiO<sub>2</sub>/PDMS 复合材料的导热系数, 探究了 H-SiO<sub>2</sub> 微球的含量和  $r/R$  对复合材料导热系数的影响. 通过与中空微球/聚合物复合材料导热系数的理论模型计算结果相比较, 证实了只有当 H-SiO<sub>2</sub> 具有完整结构且  $r/R$  高于 0.963 时, 其添加到 PDMS 中才能降低复合材料的热导系数, 且下降程度随 H-SiO<sub>2</sub> 含量增加而增大, 从而提高复合材料的隔热性能. 与此同时, 当 H-SiO<sub>2</sub> 添加量在质量分数 5% 以内时, H-SiO<sub>2</sub>/PDMS 复合材料的力学性能也随着 H-SiO<sub>2</sub> 含量增加而有所增加. H-SiO<sub>2</sub> 质量分数为 5% 时, 复合材料的拉伸强度和断裂伸长率分别提高了 100% 和 360%. 本工作为高性能中空微球填充聚合物基隔热材料的设计制备提供了理论和实验指导.

**关键词:** 中空二氧化硅微球; 硅橡胶; 导热系数; 隔热材料